12-2016

Cryogenic Viscous Liquids on Icy Moons

Danielle Neighbour
University of Arkansas, Fayetteville

Cryogenic Viscous Liquids on Icy Moons

Danielle Neighbour

University of Arkansas, Fayetteville
Civil Engineering

INTRODUCTION

The study of cryogenically viscous liquids such as methane and ethane offers critical insight into the behavior of fluids on icy moons such as Saturn's moon Titan. Shrouded by a hazy hydrocarbon shield, Titan's significant nitrogen atmosphere of 1.5 bar, methane-driven hydrological cycle, and lakes and rivers are vaguely similar to our Earthly home. The European-created Huygens probe, carried by the Cassini spacecraft, arrived on Titan's surface in January 2005 [1]. Upon landing, Huygens photographed its landing site, as seen in Figure 1. The photo depicts rocklike objects, thought to be comprised of water ice sitting in a dry lake bed with diameters 15 cm (left object) and 4 cm (right object). Their rounded shape and the darkened depressions at their bases indicate erosion due to fluvial travel.

Figure 1: ESA Huygens Probe Landing Site on Titan, January 15, 2005. The rounded shape of the rocklike objects and the indentations at their bases indicate erosional activity. Credit: JPL [1].

The apparent possibility of fluvial activity in Figure 1 has inspired this research. Through analysis of the viscosity of liquid hydrocarbons mixed with organic deposits on Titan's surface, conclusions regarding the effect of sediments on fluid dynamics on planetary bodies can be obtained. These organic deposits, called tholins, are produced in Titan's upper atmosphere due to methane photolysis and are believed to accumulate on the planetary body's surface [2]. They can also easily be transported by Aeolian and surface run off processes. The existence of tholin-organic mixed dunes, found by Huygens probe, implies large amount of tholin production, which likely has a strong effect on fluvial features.

An explanation of the lack of waves in Titan's lakes [3] may be found by studying the viscosity of liquid hydrocarbon-tholin simulant mixtures: if the lakes are significantly dense, waves may not exist due to high viscosity levels of lake fluids.

METHODS

Silicon dioxide nanoparticles were used to represent the tholin sediment at varying concentrations. Nanophase silica were selected as analogues for tholins due to their similarities in size, shape, and density (see Figure 2.)

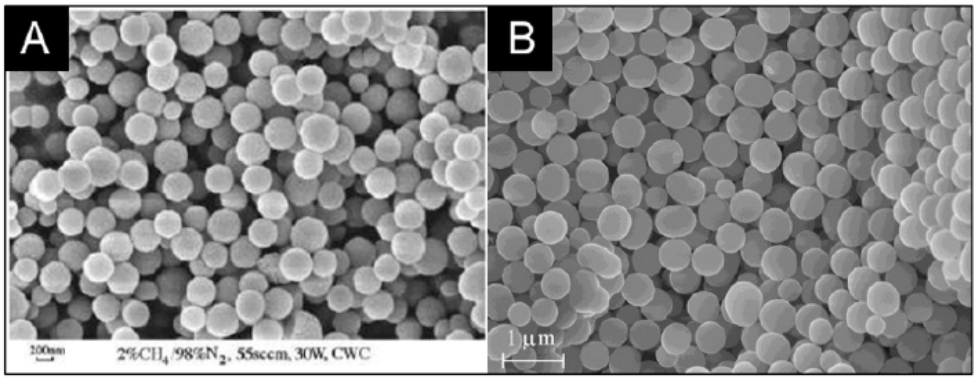

Figure 2: Electron microscope images of lab synthesized tholins (A) and nanophase silica (B). [4].

Additionally, because methane and ethane are gaseous at room temperature, liquid hydrocarbons with similar properties were used to represent methane and ethane. As polarity affects the manner in which tholins disperse, both polar (acetone, acetonitrile, diethyl ether, and ethanol) and nonpolar (hexane) liquid hydrocarbons were tested. Ether and ethanol were chosen based on their polarity and direct similarities with methane, while hexane was selected due to its non-polarity and molecular resemblance to ethane [5]. Acetone and acetonitrile were used based on their respectively unique polarities. Additionally, based on former related experimentation [5] with acetone, ether, and hexane, testing these hydrocarbons allows for verification of legitimacy of past data as

well as adding to the slim body of research on the subject. Graph 1 offers a comparison between methane, ethane, and the five hydrocarbons used for testing.

Graph 1: Comparison of critical properties between methane, ethane, and liquid hydrocarbons used in testing. [6].

Name	*Formula*	*Density (g/cm^3)*	*Viscosity (mPa*s)*	*Melt T (K)*	*Boil T (K)*	*P_{sat} (kPa)*
Methane	CH_4	0.4515	0.1934	90.69	111.51	11.7
Ethane	C_2H_6	0.6515	1.281	90.37	184.33	0.0011
Acetonitrile	C_2H_3N	0.786	0.343	227	354	9.6697
Acetone	$(CH_3)_2CO$	0.791	0.3311	179	330	24.61
Diethyl ether	$(C_2H_5)_2O$	0.7134	0.224	157	308	74
Hexane	C_6H_{14}	0.6548	0.294	178	342	17.6
Ethanol	CH_3CH_2OH	0.789	1.144	159	352	5.95

The viscosities of these selected five solutions were tested at nanoparticle concentrations from 0-20% at 5% increments over 10-minute periods. These viscosity measurements were obtained using an NDJ-1 rotary viscometer (see Figure 3), which measures the liquid viscose capacity and the viscosity of fluids from a range of 10-100,000 mPa*s [7]. During each solution's continuous 10-minute testing period, data (solution mass and dynamic viscosity) were collected every 30 seconds during the first five minutes and once a minute for the latter half of the testing period. Solution temperature before and after testing was also recorded.

Figure 3: NDJ-1 Viscometer used for testing, pictured during the calibration process. Solutions were placed on a balance for testing, allowing for collection of both solution mass and viscosity data.

After lab testing, the relationship between particulate concentration and liquid viscosity was equated using a numerical model specifically designed for Titan's fluvial topographies. This model equates the slope of the planetary surface, fluid velocity, and sediment concentration [8]. By applying this model to data obtained from the rotational viscometer,

the effect of tholin concentration on liquid methane and ethane's fluid dynamics was calculated.

RESULTS

Based on the data obtained during testing, similarities in compound viscosities became evident: acetone and acetonitrile displayed similar behaviors; diethyl ether and ethanol also exhibited related results. Hexane reacted differently than all other four liquid hydrocarbons. Results and related graphs of these groups are below. Because fluid viscosity is an exponential function of sediment concentration, all graphs include sediment concentration (kg/kg) compared to the the logarithm of dynamic viscosity (mPa*s).

Acetone and Acetonitrile. The viscosity of acetone and acetonitrile displayed no major dependence on sediment concentration. The viscosity of acetone at a 20% silica concentration varies by a percent change of 19.6% as compared to the pure compound. There was a 14.0% difference between the viscosities of pure acetonitrile and acetonitrile with a 20% silica concentration. Figures 4 and 5 display the trends exhibited by acetonitrile and acetone at increasing concentrations of nanophase silica.

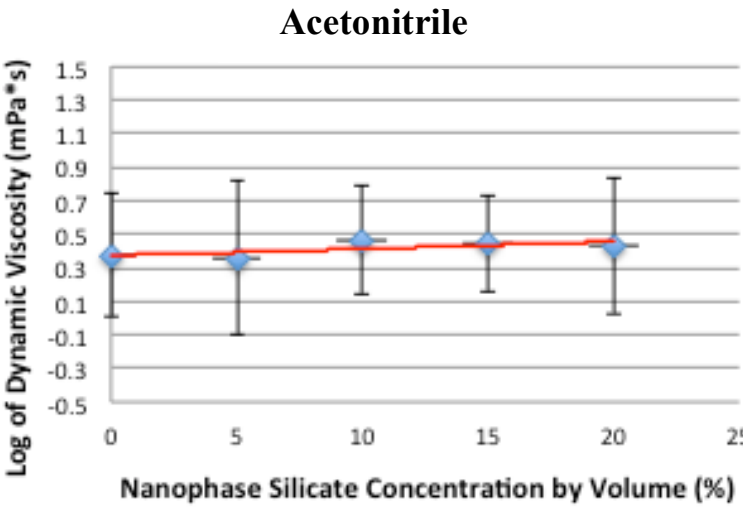

Figure 4: Percent concentration by volume of nanophase silica in acetonitrile as compared to the log of the solution's dynamic viscosity in mPa*s.

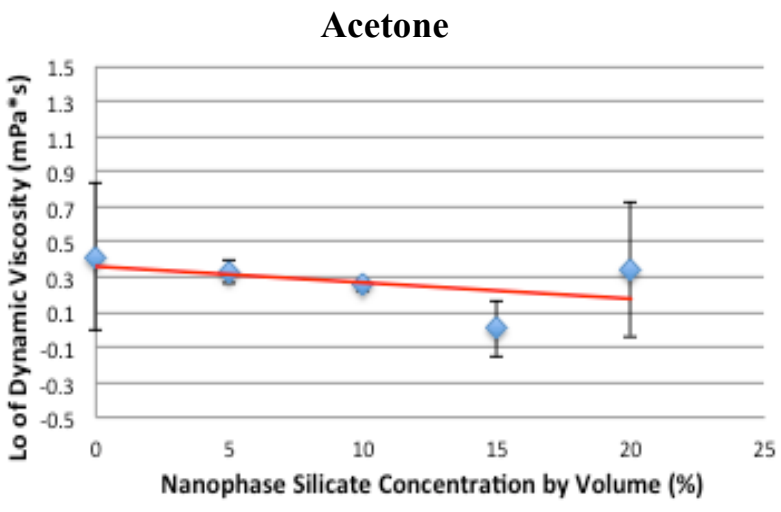

Figure 5: Percent concentration by volume of nanophase silica in acetone as compared to the log of the solution's dynamic viscosity in mPa*s.

Diethyl Ether and Ethanol. The viscosity of both ether and ethanol are moderately dependent upon silica concentration. The percent change between the viscosity of pure ether and ether at a 20% silica concentration is 76.33%. Between pure ethanol and ethanol at a 20% silica concentration, there is a 67.9% difference. Also noteworthy is the significant jump in viscosity from 15% silica concentration to 20% silica concentration for both ether and ethanol (see Figures 6 and 7). This shift is likely due to the value of viscosity being determined by liquid from percent concentrations 0-15%, while at a 20% concentration, viscosity was determined by the silica particles.

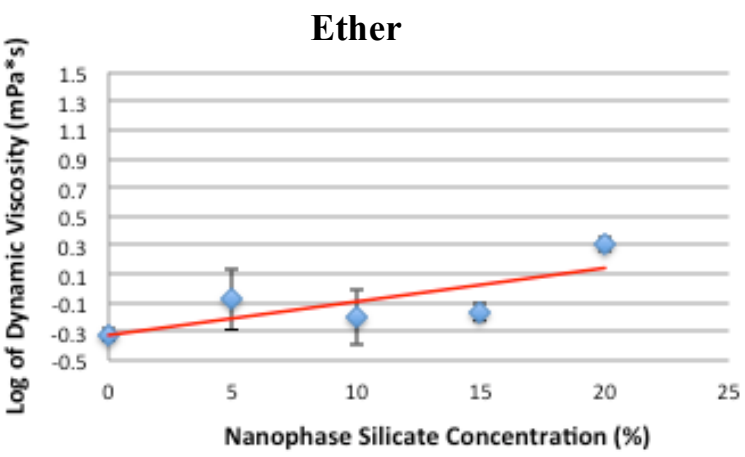

Figure 6: Percent concentration by volume of nanophase silica in ether as compared to the log of the solution's dynamic viscosity in mPa*s.

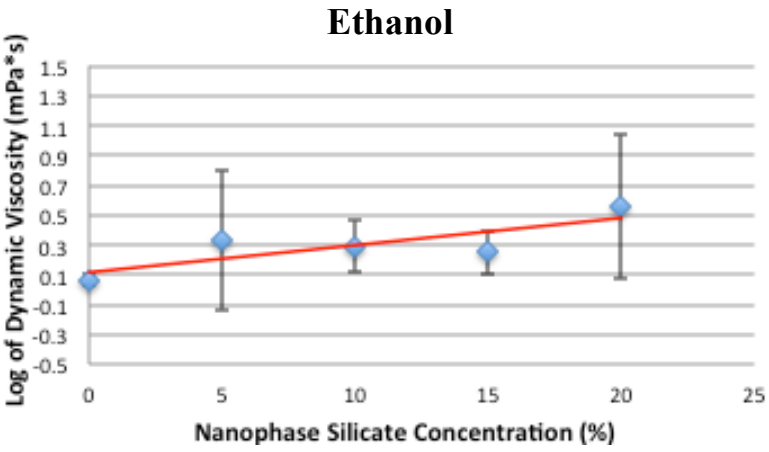

Figure 7: Percent concentration by volume of nanophase silica in ethanol as compared to the log of the solution's dynamic viscosity in mPa*s.

Hexane. Hexane's viscosity is strongly dependent on silica concentration. The percent change between pure hexane and hexane at a 20% percent concentration is 92.75%. The relationship between sediment concentration and hexane's dynamic viscosity is presented in Figure 8.

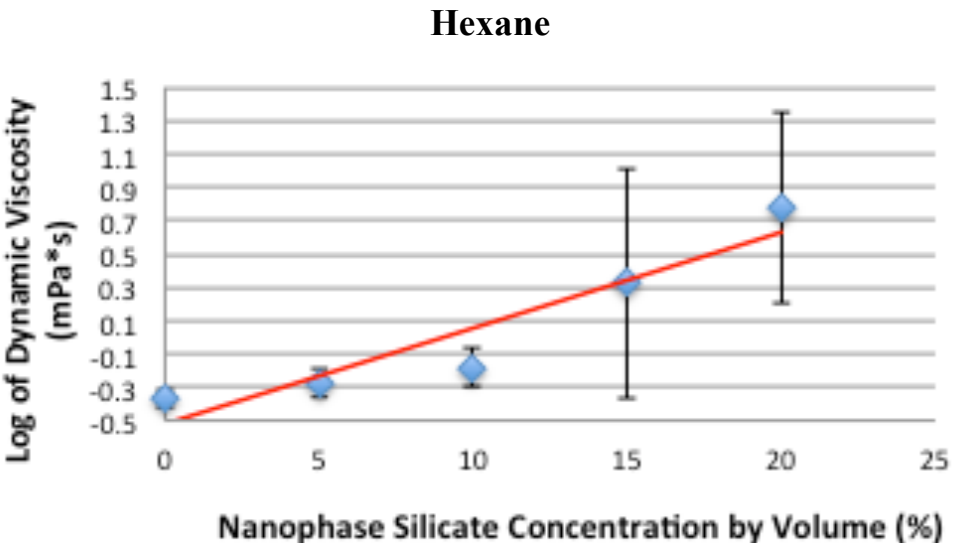

Figure 8: Percent concentration by volume of nanophase silica in hexane as compared to the log of the solution's dynamic viscosity in mPa*s.

DISCUSSION

Settling. During the testing process, settling of nanophase silica occurred in all liquid hydrocarbon mixtures; settling was most common in ethanol (see Figure 9). As settling in beakers was likely due to particle agglomeration, it is not believed to have a major affect on viscosity.

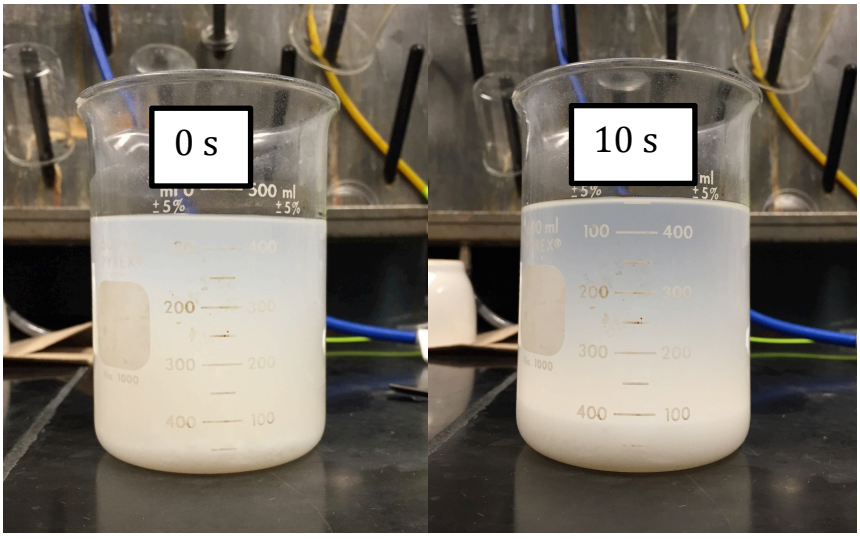

Figure 9: Nanophase silica settling in ethanol at 0 seconds after stirring (left) vs. 10 seconds after stirring (right).

Numerical Model. Because the dynamic viscosity of hexane displays a significant dependence upon sediment concentration, further analysis of hexane was performed. As methane and ethane are nonpolar compounds, liquid nonpolar hexane represents the best analogue for these hydrocarbons on Earth. In order to analyze results of viscometer testing, the following equation was used to equate dynamic viscosity (η, mPa*s) and percent concentration of nanophase silicates (C, % mL/mL) [9]:

$$\ln(\eta) = \ln(\eta_0) + \beta(C) \qquad \textbf{Eqn. 1}$$

By using the known viscosity at fixed temperatures (η_0, mPa*s), a dimensionless coefficient β was calculated. From the collected hexane data, β = 15.024. After obtaining the β value, a numerical model developed by S. Singh et al. [8] was employed to determine flow behaviors. The model utilizes the viscosity equation (Equation 1), the Darcy-Weisbach equation, and a Bernoulli fluid mechanics model to calculate flow rate. In total, the model offers two major results: an estimated average fluid velocity at Huygens' landing site and the critical boulder size, an estimation of the boulder size that could be transported by the fluid. This size is limited to a maximum of 15 cm based on boulder observations from the Huygens landing site.

Average Velocity. The first of the model's two functions, calculation of average fluid velocity, is performed with the planetary surface slope, viscosity, and sediment concentration. As the planetary surface slope varies, multiple channel sizes were used in calculations. Figures 10 and 11 on the following page display diagrams of channel cross-sections; equations 2 and 3 represent the calculations used to find average velocity in the numerical model.

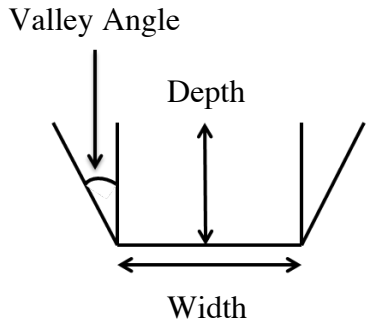

Figure 10: Cross-section of fluvial channel.

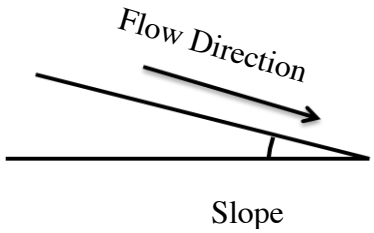

Figure 11: Cross-section of fluvial channel.

$$g(\Delta z) = \frac{fLV_{avg}^2}{2D_{hyd}} \quad \textbf{Eqn. 2}$$

$$R_e = \frac{D_{hyd}V_{avg}\rho_f}{\mu} \quad \textbf{Eqn. 3}$$

D_{hyd} = hydraulic diameter of channel
F = friction coefficient
g = gravity (1.35 m/s^2)
L = flow distance (m)
V_{avg} = fluid velocity (m/s)
Δz = elevation drop over flow distance (m)
μ = viscosity (mPa*s)
ϱ_f = fluid density (kg/m^3)
R_e = Reynold's Number

Using a density of water ice of 930 kg.m^3, a grain (average bed) roughness of 22.5 x 10^{-9} m, density of silica of 50 kg/m^3, and varying channel slopes (0.1, 0.2, and 0.3 degrees) the average velocity (m/s) at varying sediment concentrations (kg/kg) can be obtained from the model. Figure 12 displays this graph at all three channel slopes. The peak in velocity represents a flow regime transition from turbulent to laminar flow. A channel angle of 30°, channel depth of 1 m, and channel width of 5 m were used; these dimensions approximately represent the channel in which Huygens landed (see Figure 1.)

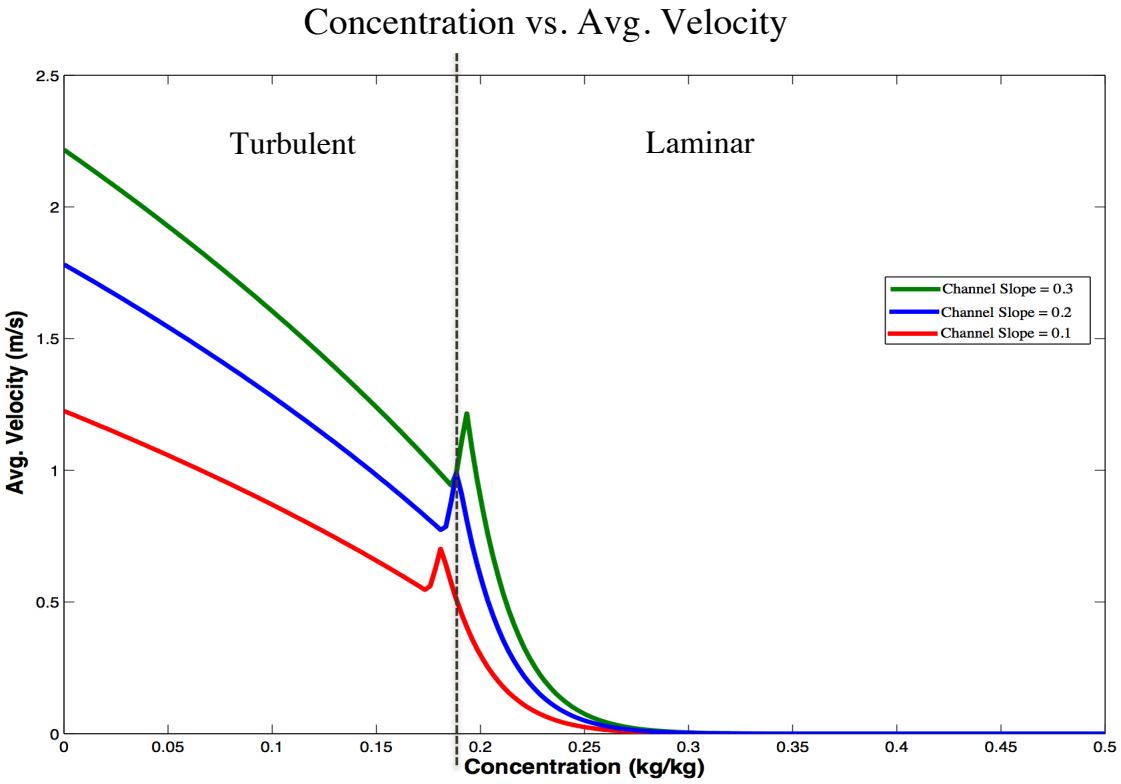

Figure 12: Concentration (kg/kg) vs. average velocity (m/s) in an average fluvial channel, modeled at Titan conditions. Note the change in turbulent to laminar flow at approximately 20% sediment concentration.

Critical Boulder Size. The second function of the numerical model, the boulder transport model, calculates the size of a boulder or cobble (boulder diameter, d, in equation 6) that could be transported at a given fluid density by equating fluid drag force (F_d in equation 4) and the boulder's weight (F_b in equation 5). The model also considers the possibility that part of the cobble is not fully submerged. Figure 13 displays the sediment concentration (kg/kg) vs. the critical boulder diameter (m) based on an average Titan fluvial channel with a channel angle of 30°, channel depth of 1 m, and channel width of 5 m as estimated from Huygens data. As with the average velocity calculation, channel slopes of 0.1, 0.2, and 0.3 degrees were considered. The transition between turbulent and laminar flow is once again visible in Figure 13 around 20% sediment concentration and is denoted with a dashed vertical line. For reference, the size range of

boulders at the Huygens landing site is denoted in red. By using the known boulder size at the Huygens landing site, the approximate sediment concentration required to transport the boulder can be determined.

$$F_d = \frac{1}{2}\rho_f C_d V_{avg}^2 S \qquad \textbf{Eqn. 4}$$

$$F_b = vg(\rho_b - \rho_f) \qquad \textbf{Eqn. 5}$$

$$d = \frac{3\rho_f C_D V_{avg}^2}{4g(\rho_b - \rho_f)} \qquad \textbf{Eqn. 6}$$

v = boulder volume (m^3)
V_{avg} = average velocity (m/s)
ρ_f = fluid density (450 kg/m^3)
ρ_b = boulder density (930 kg/m^3)
d = boulder diameter (m)
C_D = drag coefficient
F_b = weight force of boulder
F_d = drag force
g = gravity (m/s^2)
S = boulder surface area

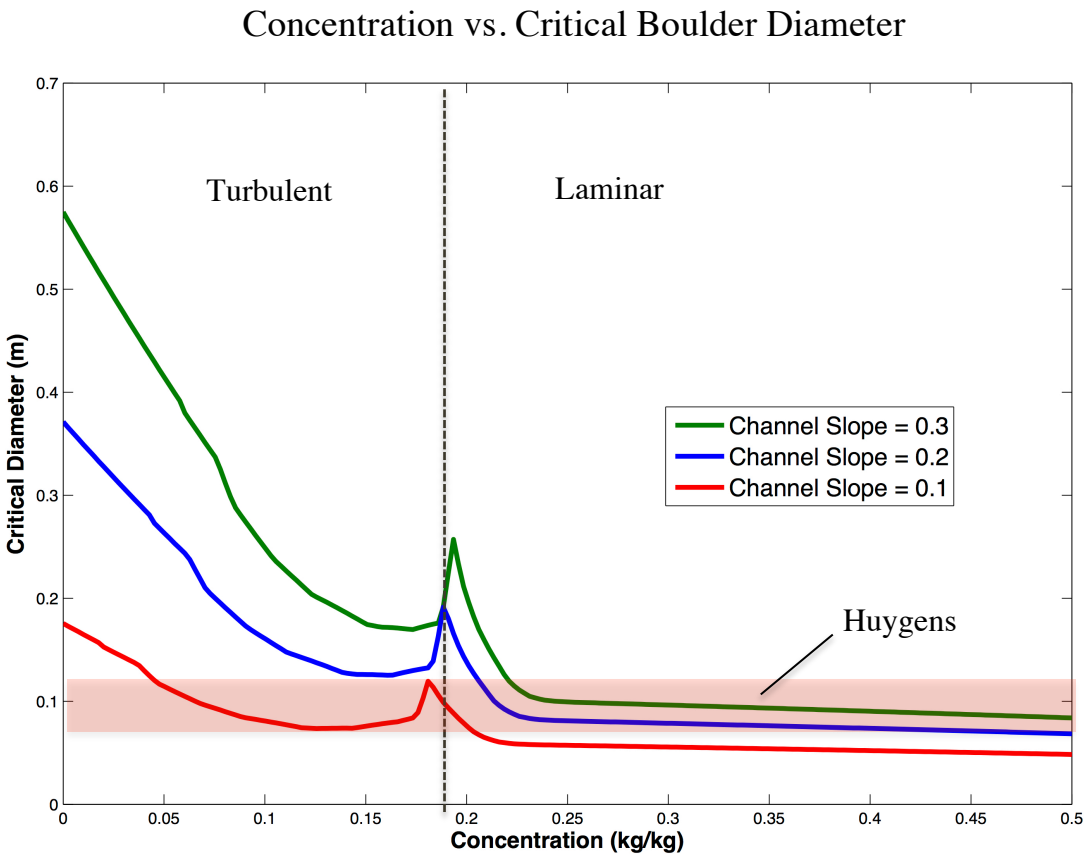

Figure 13: Sediment concentration (kg/kg) vs. critical boulder diameter (m) in an average fluvial channel, modeled at Titan conditions. Note the change in turbulent to laminar flow at approximately 20% sediment concentration and average boulder size as determined by Huygens.

CONCLUSION

Through a combination of benchtop experiments and numerical modeling, critical insight regarding average sediment concentrations, channel slopes, and velocities in Titan's fluvial channels was obtained. Based on the results of the critical boulder diameter model, the channel slope at Huygens's landing site is likely 0.1 degrees. The channel size is small (1 to 2 meters in depth, 5 to 10 meters in width). At a channel slope of 0.1 degrees, the sediment concentration is approximately 5% and flow is turbulent. Based on the results of the average velocity model, the velocity at a sediment concentration of 5% is approximately 1 m/s. This conclusion is consistent with results from Burr et al. in 2006 and 2009 [10].

In addition to conjectures from the numerical model's data, benchtop experiments displayed an increase in viscosity as sediment concentration increases in nonpolar solvents (as displayed by hexane). Titan's lakes are comprised of methane and ethane, both nonpolar compounds. As tholins are present in Titan's lakes due to fluvial and Aeolian transport, the nonpolar compounds' viscosities' strong dependence on sediment concentration could be an explanation for the lack of waves in lakes. Moreover, large concentrations of tholins would not be required to significantly change the viscosity of the liquids. Through preliminary conclusions regarding the lack of waves in Titan's lakes, sediment concentration in small channels, and the channel slope at Huygens' landing site in addition to corroborating previous conclusions regarding the average fluid velocity in small channels, this original research has continued to spur forward necessary discoveries of the characteristics of Titan.

SOURCES

[1] ESA and NASA Database, *ESA Science and Technology,* (2011).

[2] N. Sarker, et al., *Astrobiology*, 3.4 (2004) 719-726.

[3] Hayes, A., et al, *Icarus*, 225 (2013) 403-412.

[4] Dong Jane, Hee. *Aerosol Science and Technology*, 30.5 (1999) 477-488.

[5] Brophy, B., Singh, S., & Chevrier, V. (2014). *Effect of Sediment Concentration on Titan Fluid Dynamics.*

[6] W.L. Jorgensen, et al. *J. Am. Chem. Soc.* 106.22 (1984) 6638-6646.

[7] Operation Manual. NDJ-1 Viscometer (Comp.), 1.1 (2012) 1-5.

[8] S. Singh and V. F. Chevrier. In prep. (2016).

[9] H.B. Jenkins, M. Yizhak, *Chem. Rev.,* (1998) 2695-2724.

[10] Burr et al., *Icarus*. 181.1 (2006) 235-242.